NeuroImage **12,** 173–183 (2000)
doi:10.1006/nimg.2000.0604, available online at http://www.idealibrary.com on IDEAL®

Nonlinear Regression of Functional MRI Data: An Item Recognition Task Study

F. Kruggel, S. Zysset, and D. Y. von Cramon

Max-Planck-Institute of Cognitive Neuroscience, Stephanstraße 1, 04103 Leipzig, Germany

Received September 13, 1999

A classical item-recognition task was used to examine human verbal working memory in an event-related functional MRI (fMRI) study. A highly flexible experimental design incorporated a broad variation of memory load and delay time. This design allows for only three or four repetitions per stimulus condition. In a first step, linear regression analysis was applied to locate functional activation in the fMRI data. As a second step, the time course of the hemodynamic response (HR) was analyzed using nonlinear regression, which served to quantify the dependency between HR shape properties and stimulation conditions in several regions-of-interest. On the basis of this study, a closer description of the frontoparietal network involved in verbal working memory was possible. © 2000 Academic Press

Key Words: **fMRI; item-recognition; verbal working memory; hemodynamic modeling; nonlinear regressions.**

INTRODUCTION

The goal of this paper is to demonstrate the usefulness of a quantitative analysis of functional MRI (fMRI) data by nonlinear regression. Shape parameters of the hemodynamic response (HR) are derived by trial-wise modeling the fMRI time-series in regions-of-interest (ROI), and quantitative relationships between the shape parameters and the stimulation context are obtained from the regression analysis. In addition to the activation amount, the temporal behavior of activated areas on parameters of the experimental stimulation is quantified as well, which allows establishing a closer link to behavioral reaction times. As a corollary of embedding the quantitative analysis in a regression context, it is possible to revise the experimental design for a higher flexibility. Meaningful results may be achieved from only three or four repetitions of a given stimulus condition, which is a desired feature for cognitive experiments. For this demonstration, we selected a classical item-recognition task to study working memory (WM) (Sternberg, 1966), and varied three experimental scales independently: the delay length over which information had to be maintained in memory (a continuous variable), memory load (a discrete variable), and a hit/foil manipulation (a binary variable).

It appears useful to briefly review recent results from functional imaging studies in WM (for a review, see (Smith *et al.*, 1998)), which suggest a rough neural architecture of verbal WM. The system may involve at least three components (Goldman-Rakic and Friedman, 1991): (1) a phonological rehearsal component mediated by left-hemisphere frontal speech regions, including BA 44 and the inferior and superior aspects of BA 6 (Awh *et al.*, 1996; Paulesu *et al.*, 1993), (2) a storage buffer mediated by left superior parietal cortex (BA 40) (Awh *et al.*, 1996; Paulesu *et al.*, 1993), and (3) executive components mediated by the dorsolateral prefrontal cortex (PFC, BA 9/46) (D'Esposito *et al.*, 1995; Rypma *et al.*, 1999a), which was active in the *n*-back memory conditions and may reflect the need to temporally code the items in these conditions. Increasing the memory load in a item-recognition task (Rypma *et al.*, 1999a; Rypma and D'Esposito, 1999b) led to an enhanced activation in the inferior frontal gyrus (bilateral BA 44/45) and activation of additional dorsal PFC (bilateral BA 8, 9, 46, and 10). Variation of the delay length over which information had to be maintained led to an increased activity of the left middle frontal gyrus (BA 9), left inferior frontal gyrus (BA 44), and the left superior parietal lobule (Barch *et al.*, 1997).

Most of these previous studies were conducted as blocked experiments and thus limited to incorporating only a few different experimental conditions, either in memory load (e.g., Braver *et al.*, 1997; Cohen *et al.*, 1997; Rypma *et al.*, 1999a) or in delay time (Awh *et al.*, 1996; Barch *et al.*, 1997). Two issues are still controversial: (1) Does the activation amount (linearly) increase with memory load in the dorsolateral and ventrolateral PFC (Braver *et al.*, 1997) or are additional areas in the dorsolateral PFC switched on in high-load conditions (Rypma *et al.*, 1999a)? (2) Is there a delay-related activation increase in the dorsolateral PFC

1053-8119/00 $35.00

(Barch *et al.*, 1997) or a sustained activation (Cohen *et al.*, 1997; Courtney *et al.*, 1997)? In addition, we were interested how much differences in behavioral reaction times between conditions were reflected in the time course of the HR.

Event-related experimental designs allow a highly variable, randomized presentation of stimuli using orthogonal variations of memory load and delay interval. Experimental manipulations from a series of previous studies were combined in a single design here. Modeling the observed HR time course yields quantitative parameters of the brain's response to a given stimulus. For each activated region, estimates related to the activation amount (called "gain" here), the time-to-maximum ("lag") and the activation duration ("dispersion") are obtained for both cue and probe phases of an item recognition task. By relating these HR shape parameters to stimulation parameters a better understanding of the brain's network involved in human working memory may be achieved. Translating the questions posed above into this framework: (1) Does an increasing memory load lead to a (linear) increase in the activation amount (i.e., the gain) of prefrontal areas? (2) Does an increasing delay time lead to an increasing gain of the probe phase? (3) It is possible to relate behavioral reaction times to the lag of the probe phase?

The present study was performed to demonstrate the advantages of linking a highly variable experimental design with a fine-grained analysis of the hemodynamic response observed in fMRI and thereby tries to contribute to the understanding of WM function.

METHODS

Subjects

Seven right-handed subjects (ages 21–24) were recruited from the undergraduated campuses of the University of Leipzig. Subjects were excluded if they had any medical, neurological, or psychiatric illness or if they were taken any type of prescribed mediation. All subjects gave informed consent. All subjects were pretrained to assure familiarity with the task prior to scanning.

Behavioral Task

Subjects performed an item-recognition task (Sternberg, 1966). The task included a series of discrete trials. Each trial consisted of a list of uppercase target (3, 4, 5, or 6) letters, presented simultaneously for 2 s, followed by a variable blank delay period (2.0 s, 3.2 s, 4.1 s, 5.2 s, 6.2 s, 7.0 s), during which subjects had to remember the letters. After this delay a probe letter was displayed for 1 s. Subjects were asked to respond if the probe letter belonged to the previously presented list ("hit" condition: button press with their right index finger) or not ("foil" condition: button press with their right middle finger). A variable intertrial interval followed to complete a single trial of a constant duration of 18 s. Forty-eight trial combinations (4 (set sizes) $\times$ 6 (delay length) $\times$ 2 (hit/foil manipulation)) were presented randomly in a single run. Five subjects completed four runs, the other two completed three runs.

MRI Technique

Imaging was carried out on a 3.0 T Bruker Medspec 100 scanner (Bruker GmbH, Karlsruhe, Germany) equipped with a fast gradient system for echo planar imaging. A birdcage radiofrequency coil was used as a receiver. High-resolution axial T1-weighted images were obtained in every subject. A gradient-echo, single-shot, echo-planar sequence (TR = 1000 ms, TE = 40 ms) was used to acquire data sensitive to the blood-oxygen level dependent effect. Eight slices parallel to the AC-PC plane were recorded at a resolution of 3.8 $\times$ 3.8 $\times$ 5 mm with a 3-mm gap between slices. Subjects view a backlit projection screen from within the scanner tunnel through a set of mirror glasses.

Data Analysis

Off-line data analysis was carried out on a SGI Origin 2000 (Silicon Graphics, Mountain View, CA) using the BRIAN software system (Kruggel and Lohmann, 1996). Data analysis consisted of a series of steps: preprocessing, activation detection using voxel-wise linear regression, selective averaging of HRs in regions-of-interest (ROIs), and shape analysis of the hemodynamic response by nonlinear regression. These steps are now described in detail.

A standard *preprocessing* scheme was applied to the raw fMRI datasets (Kruggel *et al.*, 1998): In subsequent MR scans of a subject, MRI data at the same anatomical position may be subjected to a different intensity scaling during the signal collection and transformation steps. Data were linearly rescaled to achieve the same mean intensity across scans, and scans were concatenated to yield a single 3-D data set, where two dimensions correspond to the image plane, the third dimension to time. Small body movements were corrected by registering images in the time series using two translational and one rotational parameter. To correct for slow fluctuations of the baseline intensity, the baseline was estimated using voxel-wise low-pass filtering in the temporal domain with a cutoff frequency of 1.5 times of the trial length (0.037 Hz). The estimated baseline was subtracted from the original data. To reduce the amount of high-frequency components of physiological and system noise, data were finally low-pass filtered in the temporal domain using a cutoff frequency of 0.38 times of the trial length (0.26 Hz).

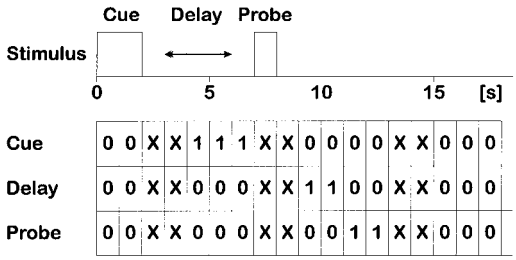

FIG. 1. Stimulation scheme (top): during the cue phase, a set of letters was presented for 2 s, followed by a variable delay time, followed by presentation of a single letter (probe phase) for 1 s. The length of an experimental trial was fixed at 18 s. The corresponding regressors for the three phases and an example delay time of 5 s are shown below. Each entry corresponds to an interval of 1 s, for which a set of fMRI slices was obtained. Entries marked as 0 correspond to baseline, 1 to activated state, X were excluded from evaluation. Regressors were shifted in time by 5.5 s in order to take the lag of the hemodynamic response into account.

The next step consisted of the *detection of activated areas* in the brain using linear regression analysis. Regressors corresponding to the cue, delay, and probe phase were constructed (see Fig. 1) to ensure orthogonality: time steps 0–1 were coded as baseline, steps 4–6 as activated for the cue regressor, steps 9–(5 + delay time) as activated for the delay regressor, and steps (6 + delay time)–(7 + delay time) as activated for the probe regressor. Two time steps around the cue phase (2–3, 7–8) and two steps following the probe phase ((8 + delay time)–(9 + delay time)) were excluded. Any remaining time steps were coded as baseline. Functional activation was detected by performing voxel-wise multivariate regression with these regressors (Rajapakse *et al.*, 1998), conversion of the *F* values into *z* scores, while taking temporal autocorrelations into account (Rajapakse *et al.*, 1998), thresholding of the corresponding *z* score map by a threshold of 3, and assessment of the activated regions for their significance on the basis of their spatial extent (Friston *et al.*, 1994).

To study the time course quantitatively in the subject group, we defined regions-of-interest (ROIs) as the six most highly activated 4-connected voxels around local maxima in the individual *z* score maps. We selected 7 ROIs that were found at homologous anatomical sites in at least 5 of the 7 subjects incorporated in this study. ROIs at their prototypical locations are shown in Fig. 3 and listed in Table 1.

Selective averaging (Dale and Buckner, 1997) was used to visualize the temporal properties of the HR time course in different ROIs. We formed averages within ROIs defined above and across all trials of the same delay time manipulations.

To describe HR *shape properties* quantitatively with respect to stimulation parameters, we used a nonlinear regression analysis (Seber and Wild, 1989). This model was described elsewhere (Kruggel and von Cramon, 1999a), so we deliberately keep the discussion short here.

TABLE 1

Talairach Coordinates of ROIs and Their Participation in the Cue, Delay, and Probe Phase, as Measured by the Average *z* Score within ROIs and across Subjects

ROI	Anatomical site	Brodmann area	Talairach coordinates		
MFG_L	Left middle frontal gyrus	BA 6/44	−43	40	28
IPS_L	(Banks) of the left inferior precentral sulcus	BA 6/44	−45	2	28
IPS_R	(Banks) of the right inferior precentral sulcus	BA 1/2/3	45	2	28
SIP_L	(Banks) of the left sulcus intraparietalis	BA 9/46	−40	−55	28
SPC_R	Right superior parietal cortex	BA 5	22	−70	36
preSMA	Pre-supplementary motor area	BA 6	− 3	−3	50
MC_L	Left motor cortex	BA 4	−28	−30	50

	Average *z* score			Regression coefficients			
ROI	Cue	Delay	Probe	Cue	Delay	Probe	Comparison
MFG_L	11.65	7.82	8.42	0.40	0.31	0.28	C = D = P, C = P
IPS_L	16.99	11.52	10.42	0.45	0.29	0.24	C > D = P, C > P
IPS_R	14.48	2.64	4.11	0.77	0.07	0.14	C > D = P, C > P
SIP_L	14.32	5.34	10.83	0.50	0.13	0.35	C > D < P, C > P
SPC_R	13.64	0.71	4.63	0.77	0.02	0.20	C > D < P, C > P
preSMA	13.67	5.80	10.61	0.43	0.17	0.38	C > D < P, C > P
MC_L	3.74	2.76	14.14	0.10	0.09	0.79	C = D < P, C < P

Note. Regression coefficients for each phase were divided by the sum of all three coefficients (see Fig. 3 for an example map). The last column lists the relative activation of ROIs during the three phases (single sided *t* tests of individual *z* scores, equal variance, $P < 0.05$), e.g., "C > D" denotes significant greater activation during the cue vs the delay phase.

We consider acquired functional data $\mathbf{y}$, collected at $k = 6$ voxel sites of predefined ROIs throughout $l = 18$ time steps of $m = \{144, 192\}$ trials. Functional data are modeled as a sum of a deterministic function $g(\cdot)$ and a stochastic part $\boldsymbol{\epsilon}$:

$$\mathbf{y} = g(\mathbf{t}, \boldsymbol{\beta}) + \boldsymbol{\epsilon}, \tag{1}$$

where $\mathbf{t}$ corresponds to the discrete time steps and $\boldsymbol{\beta}$ to the p-dimensional vector of model parameters. For this experiment, $g(\cdot)$ corresponds to a sum of three Gaussian functions, one for each experimental phase (cue, delay, and probe):

$$g(t, \boldsymbol{\beta}) = \beta_0 \exp\left[-\frac{(t-\beta_2)^2}{2\beta_1^2}\right] + \beta_3 \exp\left[-\frac{(t-\beta_5)^2}{2\beta_4^2}\right] + \beta_6 \exp\left[-\frac{(t-\beta_7)^2}{2\beta_8^2}\right]. \tag{2}$$

We denote the $p = 9$ components of $\boldsymbol{\beta}$ as $\beta_{\{0,3,6\}}$: gain (the "height" of both HRs), $\beta_{\{1,4,7\}}$: dispersion (proportional to the duration of the HRs), $\beta_{\{2,5,8\}}$: lag (the time delay from stimulation onset to the HR maximum). Note that parameters β are functions of the stimulation parameters of a given trial.

We assume that the stochastic part is independent of the signal and stationary with respect to time, and its elements are normally distributed with a nonsingular covariance matrix $\mathbf{V}$: $\boldsymbol{\epsilon} \sim N_n(0, \mathbf{V})$, where $n = k * l * m$ corresponds to the number of data points. For reasons of simplicity, we set $\mathbf{V} = \mathbf{I}$ in this study. A more advanced formulation may incorporate AR(1) autocorrelation in time and space (Kruggel and von Cramon, 1999a).

We find the ML estimate $\hat{\boldsymbol{\beta}}$ of our model parameters as the vector $\boldsymbol{\beta}$ that minimizes the quantity:

$$\arg\min_{\beta}(\boldsymbol{\epsilon}^T \mathbf{V}^{-1} \boldsymbol{\epsilon}), \quad \text{where } \boldsymbol{\epsilon} = \mathbf{y} - g(\mathbf{t}, \boldsymbol{\beta}). \tag{3}$$

This nonlinear minimization problem was solved using Powell's algorithm (Press *et al.*, 1992).

Using a first-order linear model, we can derive confidence limits for the estimation from the inverse of the Fisher information matrix $\mathbf{F}$:

$$\hat{\boldsymbol{\beta}} \sim N(\boldsymbol{\beta}, \mathbf{F}_\beta^{-1}), \quad \text{where } \mathbf{F}_\beta = \mathbf{G}_\beta \mathbf{V}^{-1} \mathbf{G}_\beta^T, \tag{4}$$

and $\mathbf{G}_\beta$ denotes the Jacobian matrix of $g(\cdot)$ with respect to $\boldsymbol{\beta}$. A simple measure for the goodness-of-fit (GOF) is given by:

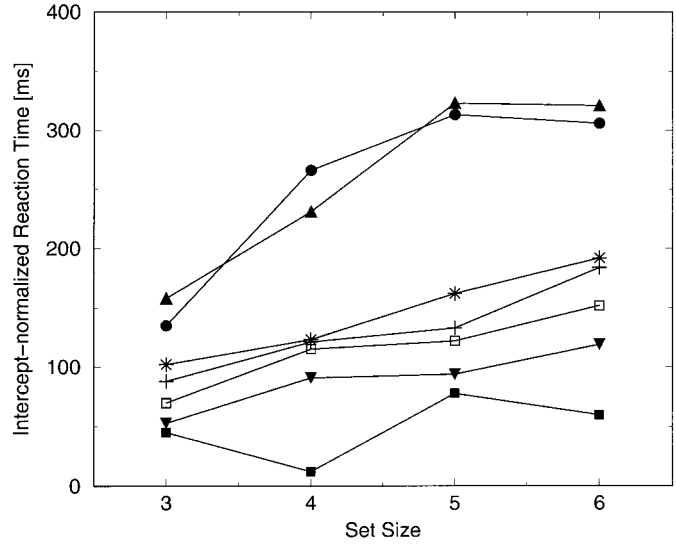

FIG. 2. Differences in individual RT slopes are found in intercept-normalized reaction times.

$$GOF = 1 - \frac{\boldsymbol{\epsilon}^T \mathbf{V}^{-1} \boldsymbol{\epsilon}}{\mathbf{y}^T \mathbf{V}^{-1} \mathbf{y}}, \quad \text{with } GOF \in [0, 1] \tag{5}$$

and 1 denoting a perfect fit. A more complex measure is given for the F statistics (Seber and Wild, 1989):

$$F_{p,n-p} \sim \frac{(n-p)}{p} \frac{\boldsymbol{\epsilon}^T \mathbf{P} \boldsymbol{\epsilon}}{\boldsymbol{\epsilon}^T (\mathbf{I}_n - \mathbf{P}) \boldsymbol{\epsilon}}, \text{ using } \mathbf{P} = \mathbf{G}_\beta \mathbf{F}_\beta^{-1} \mathbf{G}_\beta^T, \tag{6}$$

where n corresponds to the number of data points, p to the number of parameters, and $\mathbf{I}_n$ is the (n, n) identity matrix.

RESULTS

Behavioral Data

Reaction times (relative to the probe phase) and responses were recorded along with the stimulation. Results for all subjects were pooled, incorrect ($N = 34$) and missed ($N = 20$) responses were excluded from a total of $N = 1244$ trials (4.3%). No significant differences in the rate of incorrect or missed responses were found between subjects and experimental conditions. Using multivariate linear regression, the reaction time (RT) intercept was found at 835 ± 47 ms, with a RT increase per set item of 34.8 ± 7.9 ms and a RT decrease per second delay time of −15.9 ± 5.2 ms ($R^2 = 0.027$, $P < 0.001$). Hits were −48.0 ± 17.9 ms faster than foils ($P < 0.01$). RTs were independent from the experimental time (trial number). RT slopes with set size varied considerably between subjects (see Fig. 2). To better compare between the individual RT slopes, a

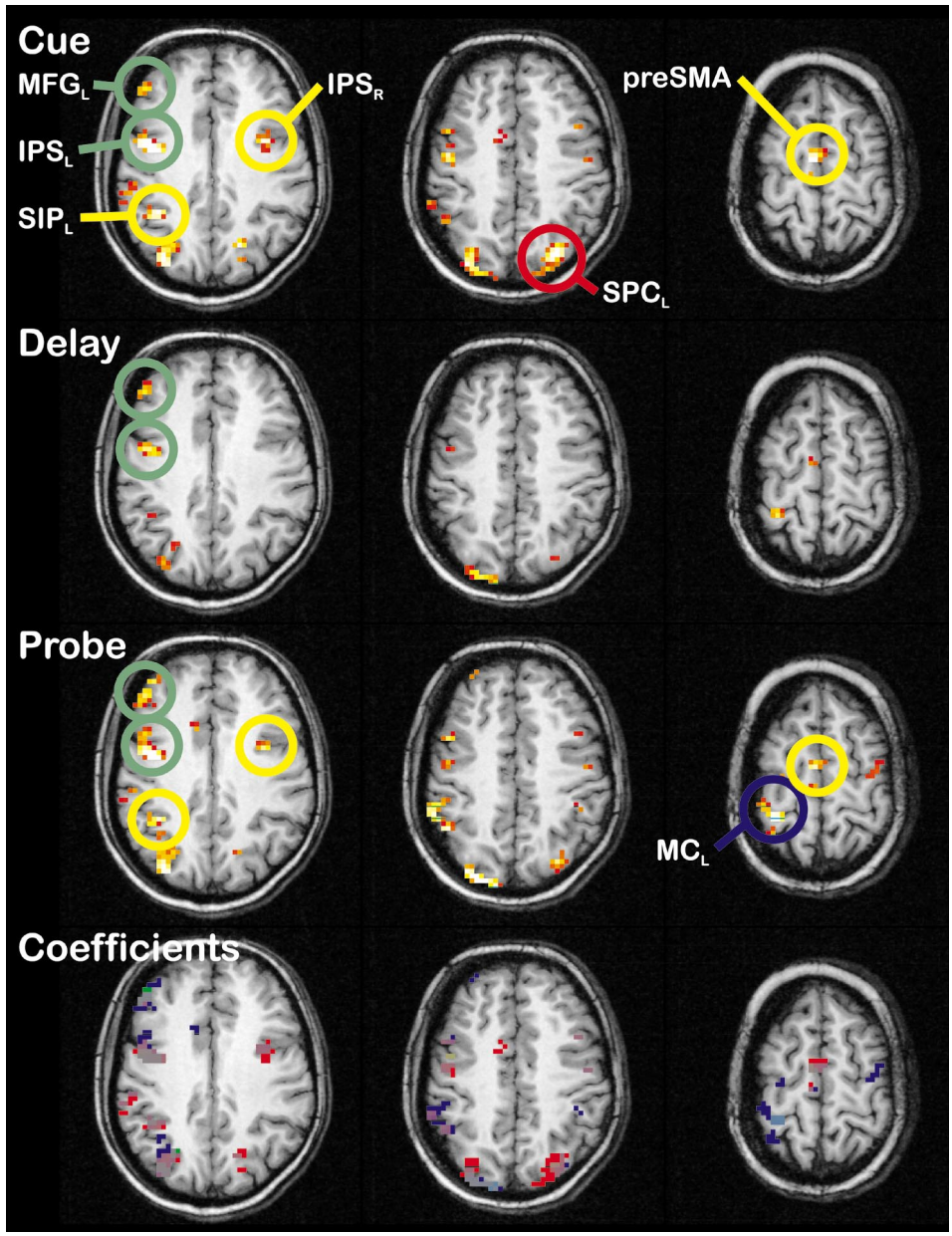

FIG. 3. Univariate regression analysis in a sample subject: significantly activated regions related to the cue phase (top), delay phase (2nd row), and probe phase (3rd row). In the bottom row, properties of ROIs from Table 2 were color-coded by their amount of contribution (red, cue phase only; blue, probe phase only; yellow, cue and probe phases; green, all three phases).

linear regression RT vs set size was computed for each subject. The individual intercept of the regression line was subtracted from the RTs, which were averaged within a given subject and experimental set size condition.

fMRI Data Analysis

Prototypical results from linear regression analysis are shown in Fig. 3, and anatomical sites of selected ROIs are compiled in Table 1. In order to determine the relative contribution of ROIs during the three experimental phases, z scores within individual ROIs were compared between phases using t tests (single-sided, equal variance, $P < 0.05$). Four different patterns were observed: ROIs contributing predominantly either to the cue phase (IPS_R) or to the probe phase (MC_L), ROIs contributing to the cue and probe phases (SIP_L, SPC_R, $preSMA$), while ROIs MFG_L and IPS_L were active in all three phases.

Selective averaging of HRs obtained under the same delay time manipulation confirmed that *all* ROIs exhibit two peaks in their time course (see Fig. 4 for an

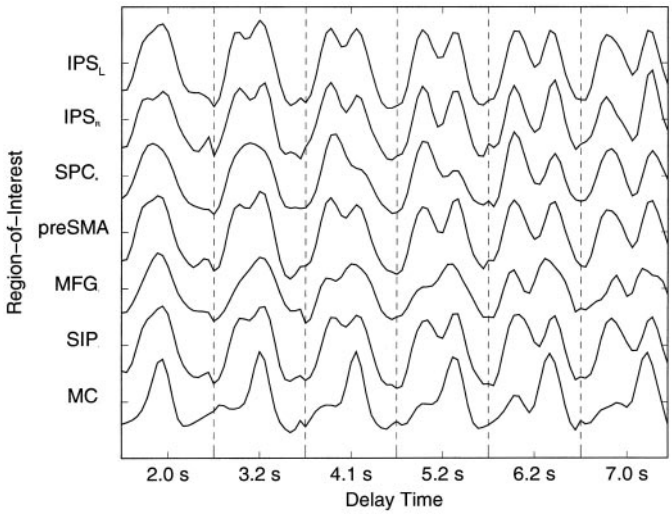

FIG. 4. Averaged time courses of the hemodynamic response from a sample subject for ROIs defined in Table 1, selected from trials of the same delay time. All regions were active in both phases of a trial.

example result). *All* regions were active during the cue and probe phase, although the activation amount in both phases differed from region to region and corresponded to the results from regression analysis compiled in Table 1. Due to the smoothness of the HR, all activations overlapped strongly for delay times of less than 4 s. The least decrease during the delay phase was found for ROI MFG_L (see Fig. 4).

To perform a quantitative analysis of the HR shape with respect to the stimulation conditions, functional models were adapted to the HR in the selected ROIs using nonlinear regression analysis. Different models were tested for the dependency of β on the stimulation parameters: The most simple model used independent gains (β_0, β_6) for cue and probe phases, a fixed dispersion ($\beta_1 = \beta_7 = 1.8$ s), and a lag time of the second phase, which followed the first one by the delay time manipulation d plus 2 s for the duration of the first stimulation phase: $\beta_8 = \beta_2 + d + 2$ s. This model resulted in GOF values (see Eq. (5)) of 0.45–0.60 for all ROIs in all subjects. Trials were excluded if subjects failed to respond or gross artifacts disturbed the HR time course. About 10–15% of the trials were rejected. Using the fitted parameters as starting values, we successively refined this model by introducing additional dependencies on the stimulation parameters. Best fits, as given by GOF values, were found for a 10-parameter model, which is explained in detail in Table 2.

As pointed out previously (Rosen *et al.*, 1998; Kruggel and von Cramon, 1999b), interindividual differences of the HR parameters were much higher than within-subject variances. For homologue regions of different subjects, the activation amount varied up to a factor of 4 and lag times up to 3 s. Thus, the nonlinear model was computed for each subject separately, and parameters were then averaged across the group. Results are shown in Table 3a. A set of interesting ratios of these parameters were formed in order to abstract from the absolute values and thus to allow a better comparison between ROIs (see Table 3b). In addition, the influence of the experimental stimulation conditions on the HR shape parameters β_i was analyzed by

TABLE 2

Best Fitting Nonlinear Model of the Hemodynamic Response and Its Dependency on Experimental Parameters in the Item-Recognition Task Studied Here

The hemodynamic response was modeled in each trial using the following function:

$$g(t, \beta) = \beta_0 \exp\left[-\frac{(t-\beta_2)^2}{2\beta_1^2}\right] + \beta_3 \exp\left[-\frac{(t-\beta_5)^2}{2\beta_4^2}\right] + \beta_6 \exp\left[-\frac{(t-\beta_7)^2}{2\beta_8^2}\right], \quad (7)$$

where the parameters β_i depend on experimental parameters in the following way:

β_0: the gain of the first response had a constant part, but depended on the trial number t (i.e., the experiment duration) and the set size s: $\beta_0 = a_0 + a_1 * t + a_2 * s$.

β_1: the dispersion of the first response had a constant part, but is due to a slope limit of the HR, dependent on the gain of the first response. This slope limit was determined heuristically and held fixed: $\beta_1 = 1.8 + 0.050 * \beta_0$.

β_2: the lag of the first response had a constant part, but depended on the set size: $\beta_2 = a_3 + a_4 * s$.

β_3: the gain of the delay phase response is constant: $\beta_3 = a_5$.

β_4: the dispersion of the delay phase response had a constant part, but depended on the gain: $\beta_4 = 1.8 + 0.050 * \beta_3$.

β_5: the lag of the delay phase response had a constant part, but depended on the delay time: $\beta_5 = a_3 + a_4 * s + d/2 + 2$.

β_6: the gain of the second response had a constant part, but depended on the trial number and the delay time d: $\beta_6 = a_6 + a_1 * t + a_7 * d$.

β_7: the dispersion of the second response had a constant part, but depended on the gain of the second response: $\beta_7 = 1.8 + 0.050 * \beta_0$.

β_8: the lag of the second response had a constant part, but depended on the delay time, the set size and the hit/foil manipulation h: $\beta_8 = a_0 + d + 2 + a_8 * s + a_9 * h$.

Note. See Table 3 for obtained parameter values.

TABLE 3

Absolute Parameter Values a_i of the Model Described in Table 2 (top) and Ratios Related to the Experimental Manipulation (below)

Parameter	MFG_L	IPS_L	IPS_R	SIP_L	SPC_R	*preSMA*	MC_L
a_0	55.8	77.2	88.0	60.8	92.4	63.3	78.6
a_1	−0.1383	−0.1377	−0.269	−0.0979	−0.0746	−0.1715	−0.132
a_2	14.61	16.07	14.68	12.35	10.37	14.254	4.92
a_3	3.52	3.41	2.98	3.98	3.54	3.54	3.09
a_4	0.3473	0.345	0.317	0.304	0.360	0.205	0.362
a_5	22.7	14.59	5.44	8.28	6.08	21.3	3.94
a_6	97.4	94.7	86.0	97.6	83.6	133.9	119.0
a_7	3.25	3.314	5.20	1.520	2.37	1.69	4.14
a_8	0.1486	0.1341	0.239	0.1240	0.286	0.0534	0.1345
a_9	−0.353	−0.0674	−0.1489	−0.1112	−0.0828	0.0251	−0.246
GOF	0.707	0.777	0.728	0.741	0.720	0.661	0.758

Ratio	MFG_L	IPS_L	IPS_R	SIP_L	SPC_R	*preSMA*	MC_L
1 Rel. cue phase activation for 0 items: $a_0/(a_0 + a_5 + a_6)$	0.317	0.414	0.490	0.365	0.507	0.290	0.390
2 Rel. delay phase activation: $a_5/(a_0 + a_5 + a_6)$	0.129	0.078	0.030	0.050	0.033	0.097	0.020
3 Rel. probe phase activation: $a_6/(a_0 + a_5 + a_6)$	0.554	0.508	0.479	0.586	0.459	0.613	0.590
4 Cue phase activation increase per item (%): a_2/a_0	26.1	20.8	16.7	20.3	11.2	22.5	6.26
5 Rel. cue phase activation for 6 items: $a_0/(a_0 + 6 * a_2 + a_5 + a_6)$	0.816	0.931	0.981	0.809	0.849	0.681	0.536
6 Probe phase activation increase per s delay time (%): a_7/a_6	3.3	3.4	6.0	1.55	2.83	1.262	3.47
7 Activation reduction with time (%): $(a_1 * 196 * 2)/(a_0 + a_6)$	35.4	31.4	60.6	24.2	16.6	34.0	26.2

Note. Between 66 and 78% of the variance was explained by this model, and all fits were assigned as significant according to the F statistics. For a further explanation, refer to Results.

computing linear regression models using group-pooled data. Results were summarized as:

• As a first approximation, all ROIs were equally active during the cue and probe phase of a trial (Table 3a, parameters a_0, a_6, and Table 3b, rows 1 and 3). In accordance with results from linear regression, a considerable delay period activation was found in ROIs MFG_L, IPS_L, and *preSMA* (Table 3b, row 2).

• The cue phase response depended on the set size manipulation only. The highest relative gain increase per set item (Table 3b, row 4) was found for ROIs MFG_L (26%), a moderate increase for ROIs SMA_L, IPS_L, IPS_R, SIP_L (≈ 20%), and a rather small increase for ROIs SPC_R and MC_L (≈ 10%). This set size-dependent effect leads to a more profound activation of the whole frontoparietal network involved in this task during the cue phase (Table 3b, row 1 vs 5). For high memory load conditions, cue phase activations are stronger than the probe phase activations (Table 3b, row 3 vs 5).

Individual differences are further illustrated in Fig. 5, where the cue phase gain (parameter β_1) is compared with the set size for ROIs MFG_L and IPS_L.

The lag of the first response also increases with set size (a_4, +296 ± 124 ms per set item, on average across all subjects and ROIs): due to slope limits of the HR, a higher gain results in a later time-to-maximum.

• The gain of the probe phase response (see Tables 3a, a_5) was independent of the set size, but increased slightly with increasing delay time (see Table 3a, a_6 and Table 3b, row 6), which might be addressed to a "reactivation effect."

• An increasing set size led to a slightly higher lag of the probe response (Table 3a, a_8, +160 ± 78 ms on average), which is in the order of the reaction time differences found for the behavioral evaluation. In Fig. 6a, lag time slopes vs set size were shown for ROI MFG_L of different individuals.

Lags of the probe response for hits were slightly faster than for foils (Table 3a, a_9, −141 ± 125 ms on average), which was in accordance with the behavioral results. The difference is high in ROIs MFG_L (see Fig. 6b) and MC_L.

• All activations decrease with experiment time (i.e., per trial number, Table 3a, a_1). Gains reduced

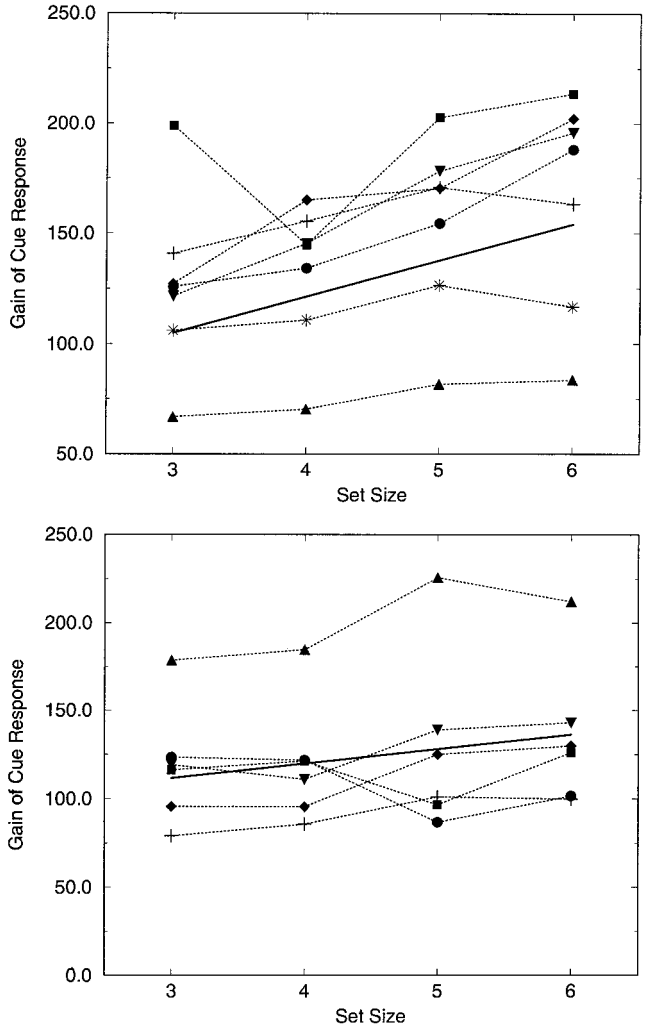

FIG. 5. The gain of the cue phase response (β_1) increased with set size in ROI IPS_L (top, +16.4 units/item, $R^2 = 0.033$, $P < 0.02$) and MFG_L (below, +8.8 units/item, $R^2 = 0.020$, $P < 0.03$). Data were pooled per subject and each line represents an individual subject.

considerably in some ROIs from the first to the last trial of the experiment (see Fig. 7 for cue phase responses of ROIs MFG_L, IPS_L). Across the group, a reduction of ≈30% was found (Table 3b, row 7), but in some ROIs of specific subjects, the reduction reached 80%.

It should be noted that time differences as given in the results section adhere to the "hemodynamic time scale." In comparison with RT differences from the behavioral results these hemodynamic time differences are longer, although a proportional relationship holds as a first-order approximation (see Fig. 8). The gain of the probe phase response did not show a significant dependency on the reaction time ($P = 0.139$).

DISCUSSION

This fMRI study demonstrated the combination of a highly flexible single-trial experimental design with a two-step data analysis using multivariate linear regression to locate functional activation related to the task and a nonlinear regression model to quantify the dependency of the HR shape on the experimental stimulation parameters. An item-recognition task was studied as an example paradigm.

This task studied requires two distinguishable groups of processes: During the cue phase and the delay period, letters need to be perceived and rehearsed. The onset of these processes are fixed in time but variable in duration (delay length) and load (set size). During the probe phase, WM contents had to be compared with the probe item, a response selected and

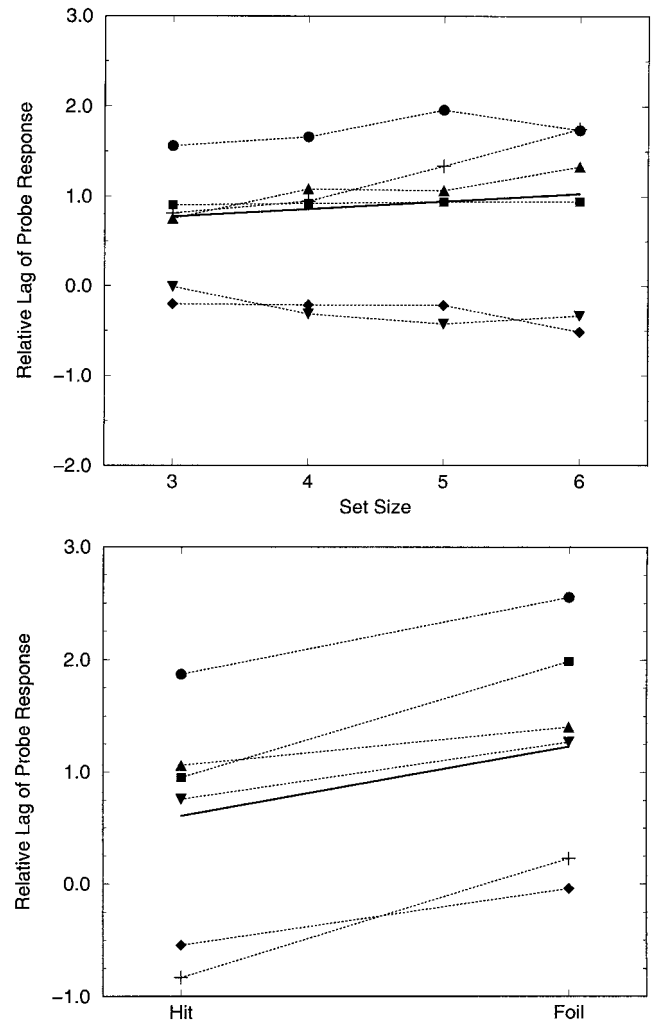

FIG. 6. The relative lag of the probe phase response ($\beta_8 - \beta_2 - t$) increased slightly with set size in ROI MFG_L (top, +85 ms/item, $R^2 = 0.034$, $P < 0.03$) and increased for foil items (below, +320 ms, $R^2 = 0.034$, $P < 0.01$). Data were pooled per subject and each line represents an individual subject.

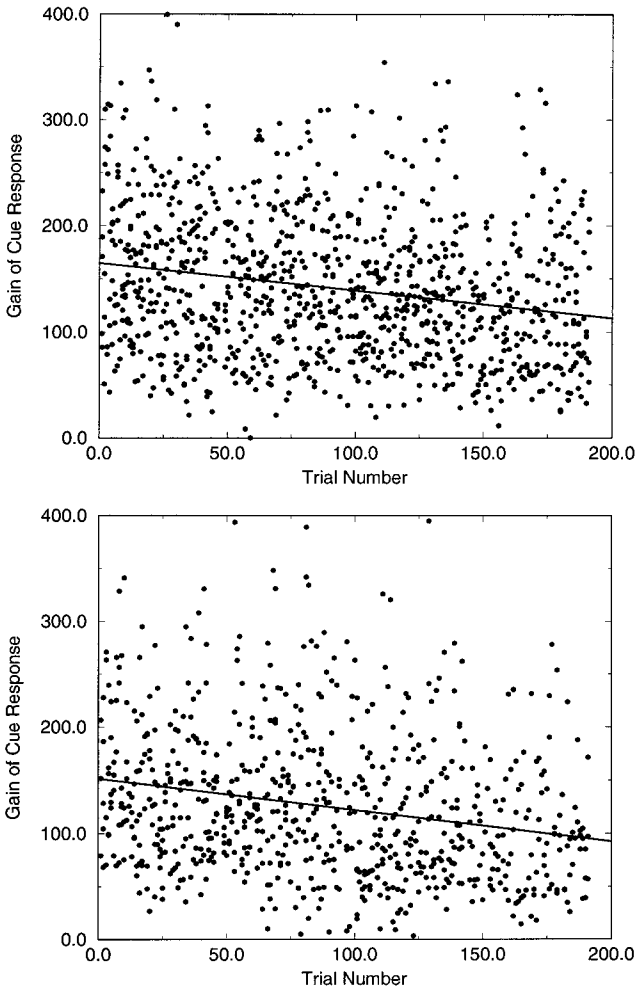

FIG. 7. The gain of the cue phase response (β_1) decreased during the experiment in ROI MFG_L (top, -0.261 units/trial, $R^2 = 0.044$, $P < 1e-11$) and IPS_L (below, -0.294 units/trial, $R^2 = 0.048$, $P < 2e-9$). Data were pooled from all subjects and all experimental conditions.

executed. The onset of these processes are temporally variable, only the matching process is load-dependent.

In order to study these processes, three experimental scales were varied independently: the delay length (a continuous variable), memory load (a discrete variable), and the hit/foil manipulation (a binary variable). Nonlinear regression served to quantify HR shape properties in terms of gain (activation amount), lag (time to HR maximum), and their dependency on parameters of the experimental stimulation.

A fronto (ROIs MFG_L, IPS_L, IPS_R, *preSMA*)-parietal (ROIs SIP_L, SPC_R) network was found to be involved during the cue and probe phase (Table 1 and Fig. 2), which is qualitatively well in accordance with recent studies of verbal working memory by positron emission tomography (Awh *et al.*, 1996; Paulesu *et al.*, 1993; Petrides *et al.*, 1993) and fMRI (Barch *et al.*, 1997; Braver *et al.*, 1997; Cohen *et al.*, 1994, 1997; Courtney *et al.*, 1998; D'Esposito *et al.*, 1998; D'Esposito *et al.*, 1999; Rypma *et al.*, 1999a; Rypma and D'Esposito, 1999b).

Quantification revealed that the cue phase activations depended on the set size manipulation only. In contrast to a recent event-related fMRI study by Rypma and D'Esposito (1999b), a load-dependent effect was found for the whole frontoparietal network during the cue phase. For subspan set sizes, an approximately linear gain increase with memory load was found (see Fig. 5 and Table 3), which was most notably in ROI MFG_L. Addressing the first question raised in the introduction, regional differences of this gain increase may explain differences in the activation pattern found in previous studies: in conventional statistics, the activation of certain regions (e.g., MFG_L) may be rated as subliminal for small set sizes and appear as "switched on" for larger sets (Table 3, row 1 vs 5). ROIs IPS_L and IPS_R were predominantly active during the cue phase, underlining their role in the encoding process.

As previously reported by Cohen *et al.* (1997) and Courtney *et al.* (1998), ROIs MFG_L, IPS_L, and *preSMA* showed significant activation during the delay phase (Table 3, row 2), which suggests involvement of these regions in maintaining information.

Probe phase responses showed a slight delay-dependent gain increase, which was most pronounced in ROIs IPS_R (6.0%), IPS_L, and MFG_L, confirming reports by Barch *et al.* (1997). Probe phase responses were independent of memory load in terms of activation amount, but showed a slight increase in lag times (e.g., Fig. 7a), which were comparable with RTs recorded alongside. This lag time dependency was most notably in ROIs MFG_L (maintaining the information), SPC_R

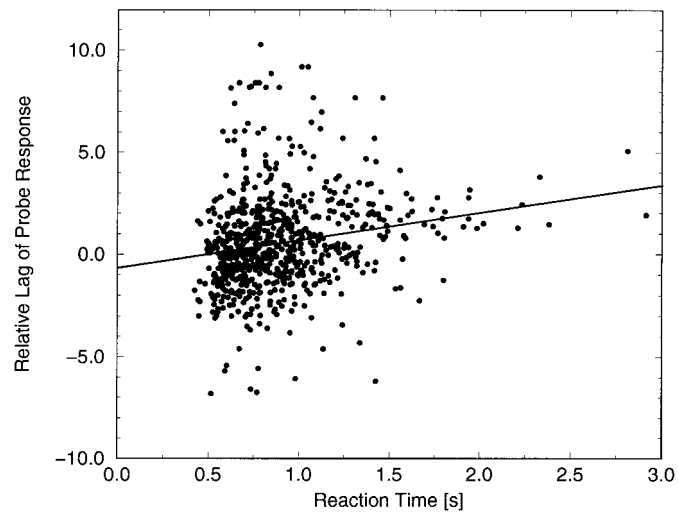

FIG. 8. The relative lag of the probe phase response ($\beta_8 - \beta_2 - t$) in relation to the measured reaction time for ROI MFG_L (lag $= -0.66$ s $+ 1.465 *$ rt, $R^2 = 0.040$, $P < 5e-8$). Data were pooled from all subjects.

(determination of familiarity), and *preSMA* (response selection). Responses in these areas were faster for hits than for foils (e.g., Fig. 7b), again with lag differences similar to RT data.

Three presumably general findings revealed by this quantitative analysis need to be emphasized:

• All activations decreased with experiment time. This effect differed by ROI and subject, but led to a gain reduction of up to 80% in some ROIs. Because similar decreases were found in other experiments as well (Kruggel and von Cramon, 1999a; Kruggel and von Cramon, 1999b), experimental time should be included as a covariate on the activation amount in quantitative analysis of fMRI data. Because no dependency of RTs on experimental time was found, this observation may be interpreted as a more efficient cortical processing requiring less neuronal space (but not necessarily less time), thus leading to a less profound BOLD effect.

• Because the HR slope is rate-limited, there is an influence of the gain on the dispersion: a stronger activation needs longer to return to base-level. Thus, the HR gain should be included as a covariate of the HR dispersion.

• As in previous studies (Kruggel and von Cramon, 1999b), we found interindividual differences in lag times of up to 3 s. We consider this finding as an argument against group-averaging fMRI data if temporal properties of the HR are of interest. Instead, we propose to extract HR shape parameters from individual fMRI data and to study (pooled) lag times for differences *relative* to the experimental stimulation.

• It is possible to relate changes in behavioral reaction times with lag time differences induced by the experimental stimulation. More specifically, an average RT increase per set item of 34.8 ms corresponded to a lag increase of 160 ms. Hits were −48.0 ms faster than foils in RT and −141 ms faster in lag times. No such relation was found between the RTs and the HR gain.

In principle, this quantitative nonlinear regression analysis may be applied *post hoc* to any event-related fMRI study. However, to gain the best profit from such an analysis, the following facts should be remembered when designing the fMRI experiment: (1) The HR dispersion σ is typically found between 2.2 and 2.8 s. Thus, two stimuli need to be separated by at least 4–5 s ($\approx 2\sigma$) to be detected as separate peaks (see also Fig. 4). To ensure that consecutive trials overlap by less that 10% in intensity, a minimum trial length of 12 s is advisable ($\approx 4\sigma$). (2) The more parameters are introduced in a HR model function, the closer it may fit the HR. In contrast, model functions with few parameters are more robust against noise and show a better optimization behavior in the fitting process. As a rough compromise, the ratio of data points recorded during an experimental trial and parameters of the HR modeling function should be at least two. Here, we recorded at 18 time points per trial and modeled HRs by a 6-parameter function. (3) HR modeling allows resolving temporal events at a higher scale than the image repetition time TR. If N trials were conducted, a temporal resolution of $\Delta t = TR/\sqrt{(N-1)}$ may be achieved and reach statistical significance. In this study, 196 trials and a $TR = 1.0$ s allowed for a maximum resolution of 71 ms.

We regard the combination of a highly flexible experimental design with a quantitative analysis by modeling the HR shape as an important advance for conducting fMRI studies:

• Meaningful results were achieved from only 3–4 repetitions of a given stimulus condition. This is a desired feature for cognitive experiments, where the similarity of repeated stimuli is of concern. It is possible to conduct experiments with true parametric variations of each variable, which closer resembles the design of behavioral experiments.

• Using individual ROIs as a basis for data analysis may appear tedious at a first glance. However, individual differences in the behavioral results, the HR properties and the cortical organization are well known and suggest to conduct the analysis on an individual level as far as possible. Because HR shape properties are obtained in parametric form, pooling within groups is easily possible, as shown in the results section.

• In comparison with the event-related analysis method described by Dale and Buckner (1997) this approach yields *quantitative* parameters that describe the HR shape. This approach makes the HR gain, lag, and dispersion accessible to statistical analysis. While the activation amount is obtained from classical linear regression analysis as well, stable and reliable quantitative estimates of temporal HR properties are not easily obtained by other methods. Brain activations may be understood in terms of activation amount (gain), duration (dispersion), and temporal order (lag). Their parametric estimates allow relating relative changes of the activation amount and HR time course to the stimulation parameters and behavioral reaction times. Our Gaussian shape model for the HR is related to the "impulse response function" introduced for analyzing event-related fMRI data by Zarahn *et al.* (1997). In contrast, our estimation model allows for *parametric* shape variations and yields quantitative estimates on a per-trial basis.

• A well thoughtout setup of the model equations for nonlinear regression (e.g., Table 2) is crucial for a successful data analysis. Knowledge about the experimental design in the form of relevant stimulation conditions is expressed here. Presumably general effects like optimization and habituation may be tested for and taken into account. Mutual dependencies of gain, lag

and dispersion, which result from physiological constraints of the neuronovascular coupling, are easily incorporated in such a model.

• Model results are obtained in the form of regression coefficients along a specific model axis (i.e., memory load, experimental time). Thus, results are based on the whole data set, and not on discrete comparisons between several experimental conditions as in more conventional designs, where analytic procedures may incorporate only subsets of the experimental data. A benefit in the form of smaller variances (or catching smaller effects) is expected.

The approach presented here achieves a much finer lever of description of a fMRI experiments and opens new perspectives for conducting fMRI experiments in cognitive neuroscience.

REFERENCES

Awh, E., Jonides, J., Smith, E. E., Schumacher, E. H., Koeppe, R. A., and Katz, S. 1996. Dissociation of storage, rehearsal in verbal working memory: Evidence from positron emission tomography. *Psychol. Sci.* **7:** 25–31.

Barch, D. M., Braver, T. S., Nystrom, L. E., Forman, S. D., Noll, D. C., and Cohen, J. D. 1997. Dissociating working memory from task difficulty in human prefrontal cortex. *Neuropsychologia* **35:** 1373–1380.

Braver, T. S., Cohen, J. D., Nystrom, L. E., Jonides, J., Smith, E. E., and Noll, D. C. 1997. A parametric study of prefrontal cortex involvement in human working memory. *NeuroImage* **5:** 49–62.

Cohen, J. D., Forman, S. D., Braver, T. S., Casey, B. J., Servan-Schreiber, D., and Noll, D. C. 1994. Activation of the prefrontal cortex in a nonspatial working memory task with functional MRI. *Hum. Brain Mapp.* **1:** 293–304.

Cohen, J. D., Perlstein, W. M., Braver, T. S., Nystrom, L. S., Noll, D. C., Jonides, J., and Smith, E. E. 1997. Temporal dynamics of brain activation during a working memory task. *Nature* **386:** 604–607.

Courtney, S. M., Petit, L., Maisog, J., Ungerleider, L. G., and Haxby, J. V. 1998. Transient, sustained activity in a distributed neural system for human working memory. *Science* **279:** 1347–1349.

Dale, A. M., and Buckner, R. L. 1997. Selective averaging of rapidly presented individual trials using fMRI. *Hum. Brain Mapp.* **5:** 329–340.

D'Esposito, M., Detre, J. A., Alsop, D. C., Shin, R. K., Atlas, S., and Grospresman, M. 1995. The neural basis of the central executive system of working memory. *Nature* **378:** 279–281.

D'Esposito, M., Aguirre, G. K., Zarahn, E., Ballard, D., and Shin, R. K. 1998. MRI studies of spatial, non-spatial working memory. *Cog. Brain Res.* **7:** 1–13.

D'Esposito, M., Postle, B. R., Jonides, J., and Smith, E. E. 1999. The neural substrate and temporal dynamics of interference effects in working memory as revealed by event-related functional MRI. *Proc. Natl. Acad. Sci. USA* **96:** 7514–7519.

Friston, K. J., Worsley, K. J., Frackowiak, R. S. J., Mazziotta, J. C., and Evans, A. C. 1994. Assessing the significance of focal activations using their spatial extent. *Hum. Brain Mapp.* **1:** 210–220.

Goldman-Rakic, P. S., and Friedman, H. 1991. Circuitry of primate prefrontal cortex, the regulation of behavior by representational memory. In *Frontal Lobe Function and Dysfunction*, Oxford Univ. Press, New York.

Kruggel, F., and Lohmann, G. 1996. BRIAN (Braim Image Analysis)—A toolkit for the analysis of multimodal brain data sets. In *Computer Aided Radiology (CAR'96)*, pp. 323–328, Elsevier, Amsterdam.

Kruggel, F., Descombes, X., and von Cramon, D. Y. 1998. Preprocessing of fMRI datasets. In *Workshop on Biomedical Image Analysis (Santa Barbara)*, pp. 211–220, IEEE Comp. Press, Los Alamitos.

Kruggel, F., and von Cramon, D. Y. 1999a. Modeling the hemodynamic response in single-trial functional MRI experiments. *Magn. Reson. Med.* **42:** 787–797.

Kruggel, F., and von Cramon, D. Y. 1999b. Temporal properties the hemodynamic response in single-trial functional MRI experiments. *Hum. Brain Mapp.* **8:** 259–271.

Paulesu, E., Frith, C. D., and Frackowiak, R. S. J. 1993. The neural correlates of the verbal component of working memory. *Nature* **362:** 342–345.

Petrides, M., Alivisatos, B., Evans, A. C., and Meyer, E. 1993. Dissociation of the human mid-dorso-lateral from posterior dorsolateral frontal cortex in memory processing. *Proc. Natl. Acad. Sci. USA* **90:** 873–877.

Press, W. H., Flannery, B. P., Teukolsky, S. A., and Vetterling, W. T. 1992. *Numerical Recipes in C*, Cambridge Univ. Press, Cambridge.

Rajapakse, J. C., Kruggel, F., Maisog, J., and von Cramon, D. Y. 1998. Modeling hemodynamic response for analysis of functional MRI time-series. *Hum. Brain Mapp.* **6:** 283–300.

Rosen, B. R., Buckner, R. L., and Dale, A. M. 1998. Event-related fMRI: past, present and future. *Proc. Natl. Acad. Sci. USA* **95:** 773–780.

Rypma, B., Prabhakaran, V., Desmond, J. E., Glover, G. H., and Gabrieli, J. D. E. 1999a. Load-dependent roles of frontal brain regions in the maintenance of working memory. *NeuroImage* **9:** 216–226.

Rypma, B., and D'Esposito, M. 1999b. The roles of prefrontal brain regions in components of working memory: Effects of memory load and individual differences. *Proc. Natl. Acad. Sci. USA* **96:** 6558–6563.

Seer, G. A. F., and Wild, C. J. 1989. *Nonlinear Regression*, Wiley, New York.

Smith, E. E., Jonides, J., Marshuetz, C., and Koeppe, R. A. 1998. Components of verbal working memory: Evidence from Neuroimaging. *Proc. Natl. Acad. Sci. USA* **95:** 876–882.

Sternberg, S. 1966. High-speed scanning in human memory. *Science* **153:** 652–654.

Zarahn, E., Aguirre, G., and D'Esposito, M. 1997. A trial-based experimental design for fMRI. *NeuroImage* **6:** 122–138.